Cancer Research

DKK2 mediates osteolysis, invasiveness and metastatic spread in Ewing sarcoma

Kristina Hauer, Julia Calzada-Wack, Katja Steiger, et al.

Cancer Res Published OnlineFirst November 30, 2012.

Title: DKK2 mediates osteolysis, invasiveness and metastatic spread in Ewing sarcoma

Authors: Kristina Hauer[1], Julia Calzada-Wack[2], Katja Steiger[2], Thomas G.P. Grunewald[1], Daniel Baumhoer[3], Stephanie Plehm[1], Thorsten Buch[4], Olivia Prazeres da Costa[4], Irene Esposito[2,5], Stefan Burdach[1], Günther H.S. Richter[1].

Institutional affiliations: [1]Children's Cancer Research Center and Department of Pediatrics, Roman Herzog Comprehensive Cancer Research Center and Klinikum rechts der Isar, Technische Universität München, 81664 Munich, Germany, [2]Institute of Pathology, Helmholtz Center Munich - German Research Center for Environmental Health, 85764 Neuherberg, Germany, [3]Bone Tumor Reference Center at the Institute of Pathology, University Hospital Basel, 4031 Basel, Switzerland, [4]Institute for Medical Microbiology, Immunology and Hygiene, Technische Universität München, 81675 Munich, Germany, [5]Institute of Pathology, Technische Universität München, 81675, Munich, Germany

Running title: DKK2 in ES pathology

Keywords: DKK2, osteolysis, invasiveness, metastasis, Ewing sarcoma

Financial support: This work was supported by grants from Technische Universität München (KKF_B08-05 to TG and A09-02 to GR); the Wilhelm-Sander-Stiftung (2009.901.1 to GHSR and SB); is part of the Translational Sarcoma Research Network supported by the BMBF (FK 01GM0870 and 01GM1104B to GHSR and SB) and Deutsche Forschungsgemeinschaft (DFG_GR3728/1-1 to TG, GHSR, and SB; DFG_GR3728/2-1 to TG). Work in IEs laboratory is supported by the National Genome Research Network (NGFNplus, 01GS0850) and in TBs laboratory by the Deutsche Forschungsgemeinschaft (SFB-TR22).

Corresponding author: Günther HS Richter, PhD, Children's Cancer Research Center and Department of Pediatrics, Roman Herzog Comprehensive Cancer Research Center and Klinikum rechts der Isar, Technische Universität München, 81664 Munich, Germany, phone: +49-89-3068-3235, fax: +49-89-3068-3791, e-mail: somagene@lrz.tum.de; guenther.richter@lrz.tum.de

Conflict of interest: The authors disclose no potential conflicts of interest.

Additional Footnotes: This work contains part of the doctoral thesis of KH;
SB and GHSR share senior authorship

Word count: 4985 (max. 5000)

Number of figures: 7 main figures/tables and 6 supplementary

Abstract

Ewing sarcoma (ES), an osteolytic malignancy that mainly affects children and young adults, is characterized by early metastasis to lung and bone. In this study, we identified the pro-metastatic gene DKK2 as a highly overexpressed gene in ES compared to corresponding normal tissues. Using RNA interference, we demonstrated that DKK2 was critical for malignant cell outgrowth *in vitro* and in an orthotopic xenograft mouse model *in vivo*. Analysis of invasion potential in both settings revealed a strong correlation of DKK2 expression to ES invasiveness that may be mediated by the DKK effector matrix metalloproteinase 1 (MMP1). Further, gene expression analyses established the ability of DKK2 to differentially regulate genes such as *CXCR4*, *PTHrP*, *RUNX2* and *TGFβ1*, that are associated with homing, invasion and growth of cancer cells in bone tissue as well as genes important for osteolysis, including *HIF1α*, *JAG1*, *IL6* and *VEGF*. DKK2 promoted bone infiltration and osteolysis *in vivo* and further analyses defined DKK2 as a key factor in osteotropic malignancy. Interestingly, in ES cells DKK2 suppression simultaneously increased the potential for neuronal differentiation while decreasing chondrogenic and osteogenic differentiation. Our results provide strong evidence that DKK2 is a key player in ES invasion and osteolysis and also in the differential phenotype of ES cells.

Introduction

Ewing sarcomas (ES) are undifferentiated bone or soft tissue tumors of enigmatic histogenesis mostly occurring in children and adolescents. Genetically, ES are defined by EWS/ETS translocations (1,2). These highly malignant tumors frequently arise in bones possibly descending from a mesenchymal stem cell in transition from an undifferentiated state to a more differentiated phenotype of the endothelial, neuroectodermal or, as hypothesized here, of the chondro-osseous lineage (2–4).

Although prognosis of patients with localized disease has markedly improved in past decades, metastatic disease – present in about 25% of ES patients at diagnosis – is usually associated with fatal outcome (5,6). Especially the development of metastases in bones is a catastrophic event in the clinical course of ES patients (5,7). Hence, there is an urgent need to understand the fundamental molecular mechanisms of ES differentiation, invasion and osteolytic tumor growth to possibly identify novel therapeutic strategies to prevent metastasis.

Previously, we described an ES-specific expression signature comprising 37 genes that are highly up-regulated or specifically expressed in ES (8). One of them is dickkopf 2 (Dickkopf, Xenopus, Homolog 2) a member of the dickkopf family. Recently, DKK2 was reported as a key player in stem cell signaling networks due to its function as a Notch signaling target (9). However, its precise cellular function remains elusive. For instance, secreted DKK2 can either function as a Wnt agonist or antagonist, depending on the cellular context and the expressed amount of its binding partner low density lipoprotein receptor-related protein 6 (LRP6) and its cofactor Kremen 2 (10–13). In the context of the Wnt/β-catenin pathway, DKK2 may promote osteoclastogenesis by enhancing the expression of osteoclast differentiation

factors, thus leading to tumor-associated osteolysis (14,15). Furthermore, Li *et al.* demonstrated that DKK2 has a role in terminal osteoblast differentiation into mineralized matrices through both canonical Wnt antagonism-dependent and -independent mechanisms (16). Based on these observations, we hypothesized that DKK2 is involved in ES invasion, osteolysis and in chondrogenic/osteogenic differentiation potential.

In the present study, we analyzed the putative oncogenic function of DKK2 in ES *in vitro* and *in vivo*. We demonstrate that DKK2 increases ES proliferation, anchorage-independent colony formation, osteolysis and invasiveness, the latter being likely mediated by MMP1. In addition, we show that DKK2 expression prevents neuronal, but in parallel enhances chondrogenic and osteogenic differentiation capacity of ES. Furthermore, DKK2 regulates the expression of different genes important for homing, invasion into bone and osteolysis, suggesting that DKK2 overexpression is a critical factor in ES malignancy, in particular bone metastasis.

Materials and Methods

Cell lines

ES lines (MHH-ES1, RD-ES, SK-ES1, SK-N-MC and TC-71) and neuroblastoma lines (CHP126, MHH-NB11, SHSY5Y and SIMA) were obtained from the German Collection of Microorganisms and Cell Cultures (DSMZ). ES line VH64 was kindly provided by Marc Hotfilder (Münster University, Germany); osteosarcoma cell lines (HOS, HOS-58, MG-63, MNNG, SaOS, SJSA01, U2OS and ZK-58) by Jan Smida and Michaela Nathrath, Institute of Pathology and Radiation Biology (Neuherberg, Germany). A673 was purchased from ATCC (LGC Standards). SB-KMS-KS1 cells and SB-KMS-MJ1 are ES cell lines that were established in our lab (17,18). Retrovirus packaging cell line PT67 was obtained from Takara Bio Europe/Clontech. Cells were maintained in a humidified incubator at 37°C in 5-8% CO_2 atmosphere in RPMI 1640 or DMEM medium (both Invitrogen) containing 10% heat-inactivated fetal bovine serum (Biochrom) and 100µg/ml gentamicin (Invitrogen). Cell lines were checked routinely for purity (e.g. EWS-FLI1 translocation product, surface antigen or HLA-phenotype) and Mycoplasma contamination.

RNA interference (RNAi)

For transient RNA interference cells were transfected with small interfering RNA (siRNA) as described previously (17). siRNA sequences are provided in the supplementary information.

Constructs and retroviral gene transfer

For stable silencing of DKK2 expression oligonucleotides were designed corresponding to the most efficient siRNA used for transient RNA interference (see supplementary information) and retroviral gene transfer was performed as described previously (17).

Quantitative RT-PCR (qRT-PCR)

Differential gene expression was analyzed by qRT-PCR using TaqMan Universal PCR Master Mix and fluorescence detection with an AB 7300 Real-Time PCR System (both Applied Biosystems) as described previously (17). A list of the assays used is provided in the supplementary information.

Flow cytometry

For DNA content, cells were fixed in ice-cold 70% ethanol at -20°C overnight and stained with propidium iodide (50mg/ml) plus RNase (5mg/ml) in PBS. The fluorescence of cells was measured using a FACSCalibur flow cytometer (BD Biosciences) and analyzed using Cellquest software (BD Biosciences).

Proliferation assay

Cell proliferation was measured with an impedance-based instrument system (xCELLigence, Roche/ACEA Biosciences) enabling label-free real time cell analysis. Briefly, 1-3x10^4 cells were seeded into 96-wells with 200µl media containing 10% FBS and allowed to grow up to 72 hours. Cellular impedance was measured periodically every 4 hours and gene knock-down was monitored by qRT-PCR.

Colony forming assay

Cells were seeded in duplicate into a 35mm plate at a density of $5x10^3$ cells per 1.5ml methylcellulose-based media (R&D Systems) according to the manufacturer's instructions and cultured for 10-14 days at 37°C/5% CO_2 in a humidified atmosphere.

In vitro invasion assay

To study cell invasion, the *BioCoat™ Angiogenesis System: Endothelial Cell invasion* was used (BD Biosciences) according to the manufacturer's instructions as described previously (18).

Western blot

Procedures were described previously (17). Following antibodies were used: anti-DKK2 (1:100; PAB3570, Abnova), anti-GAP43 (1:500; ab7462; Abcam) and horseradish peroxidase-coupled bovine anti-rabbit IgG (1:500; sc-2370; Santa Cruz Biotechnology). Equal protein loading was controlled with rabbit polyclonal to HPRT antibodies (1:500; sc20975; Santa Cruz Biotechnology).

Differentiation assay

For neuron/astrocyte-like cell differentiation, cells were cultured as already described (17) and the differentiated cells were identified by staining with an antibody directed against GFAP (BD Biosciences) and visualized with a FITC-labeled goat anti-mouse F(ab')2 fragment (Jackson ImmunoResearch Laboratories) or with an antibody against the neuronal marker GAP43 (Abcam) using western blot analysis.

Microarray data

Comparative gene expression analysis was performed as previously described (17,18) using human Gene ST arrays (Affymetrix, GSE36100). Gene set enrichment analysis (GSEA) and set-to-set pathway analyses of leading-edge genes were performed with the GSEA tool (http://www.broad.mit.edu/gsea) in default parameters (19).

Animal model

Immunodeficient Rag2$^{-/-}\gamma c^{-/-}$ mice on a BALB/c background were obtained from the Central Institute for Experimental Animals (Kawasaki, Japan) and maintained in our animal facility under pathogen-free conditions in accordance with the institutional guidelines and approval by local authorities. Immunodeficient NOD/SCID Balb/c mice were purchased by Charles River Laboratories International. Experiments were performed in 6-16 week old mice.

In vivo experiments

For the analysis of *in vivo* tumor growth and metastatic potential 1.5-3x10^6 ES cells and derivates were injected in a volume of 0.2ml into immunodeficient Rag2$^{-/-}\gamma c^{-/-}$ or NOD/SCID Balb/c mice as described previously (17,18). To examine bone invasiveness and osteolysis, mice were anesthetized with 500mg/ml Novaminsulfon (Ratiopharm) and isoflurane (Abbott). A 30-gauge needle was introduced through the proximal tibia plateau and 2x10^5 ES cells in a volume of 20µl were injected into the medullary cavity. In all experiments, tumors and affected tissues were recovered and processed for histological analyses. Intra-tibial tumor formation was monitored by X-ray radiography.

Histology

Murine organs were fixed in phosphate buffered 4% formaldehyde and embedded in paraffin. Three to five µm thick sections were stained with hematoxylin and eosin (H&E). The amount of osteoclasts was detected by tartrate-resistant acid phosphatase staining (TRAP). All sections were reviewed and interpreted by two pathologists (J.C-W. and I.E.).

Statistical analyses

Data are mean ± SEM as indicated. Differences were analyzed by unpaired two-tailed student's t-test as indicated using Excel (Microsoft) or Prism 5 (GraphPad Software); p values < 0.05 were considered statistically significant (*$p < 0.05$; **$p < 0.005$; ***$p < 0.0005$).

Results

DKK2 is highly overexpressed in Ewing sarcomas

In a previous microarray analysis, we identified *DKK2* as one of 37 genes, which were strongly up-regulated in ES compared to normal tissues (Fig. 1A) (8). To analyze specificity of DKK2 expression in ES, we tested ES cell lines against a series of different osteosarcoma and neuroblastoma cell lines. qRT-PCR revealed a high expression of DKK2 only in bone-associated tumors such as ES and osteosarcomas, but not in neuroblastomas and other small-round-blue cell tumors (Fig. 1B and supplementary Fig. S1).

Although DKK2 seems up-regulated in several pediatric bone tumors, we were curious whether DKK2 expression in ES is dependent on the expression of the oncofusion protein EWS-FLI1. Transient knock-down of EWS-FLI1 by specific siRNA did not significantly affect DKK2 expression in four ES cell lines, indicating DKK2 expression in ES to be independent of EWS-FLI1 (Fig. 1C). Furthermore, constitutive suppression of DKK2 did not influence EWS-FLI1 mRNA levels (Fig. 1D).

DKK2 increases tumor growth and metastasis *in vitro* and *in vivo*

To analyze the impact of DKK2 overexpression on the phenotype of ES, we transiently and constitutively down-regulated DKK2 in three different ES cell lines (Fig. 2A+B). Using an xCELLigence instrument, we first analyzed the effect of DKK2 knock-down on the proliferation of ES cell lines *in vitro*. Constitutive down-regulation of DKK2 revealed a significant inhibition of proliferation in A673 and SK-N-MC cells

(Fig. 2C), without significantly affecting cell cycle progression (Fig. 2D). We next tested anchorage-independent growth of stable DKK2 infectants in methylcellulose. As shown in Fig. 2E, constitutive DKK2 knock-down clearly reduced colony formation in all three ES cell lines in a dose dependent manner (Fig. 2B).

We further examined whether suppression of DKK2 in ES affects tumorigenicity and metastasis *in vivo*. We injected stable pSIREN^{DKK2}-infected A673 and SK-N-MC cells and respective controls subcutaneously into the inguinal region of immunodeficient mice and analyzed tumor growth. As shown in Fig. 3A, DKK2 knock-down clearly delayed local tumor growth in both ES cell lines in a dose-dependent manner. Similarly, suppression of DKK2 significantly reduced the number of lung metastases, when cells were injected into the tail veins of Rag2$^{-/-}\gamma c^{-/-}$ mice (Fig. 3B). Furthermore, considering in addition liver and kidney metastases, pSIREN^{DKK2} infectants revealed a strong reduction of overall metastatic potential by up to 95.8% (Table 1), suggesting a critical role of DKK2 in ES growth and metastasis.

DKK2 knock-down inhibits invasiveness regulated by MMP1 *in vitro*

To identify possible DKK2 downstream targets that are presumably involved in metastasis, we transiently down-regulated DKK2 in A673 and SK-N-MC cells (Fig. 2A) and compared their expression pattern with pSIREN^{negsiRNA} cells in a microarray analysis on human Gene ST arrays (Affymetrix, GSE36100). Considering a minimum linear fold change > ±1.5 we identified 281 differentially regulated genes of which 207 genes were down-regulated after DKK2 knock-down (Fig. 4A). Differential expression of five of these genes, which all have been reported to be involved in cellular invasiveness and migration, was confirmed by qRT-PCR (Fig. 4B). The only up-

regulated gene of these five genes is the key cell-cell adhesion molecule *E-Cadherin* (*CDH1*), which is a well-established antagonist of invasion and metastasis (20). The four down-regulated genes are the *integral cell membrane glycoprotein CD44*, which has a postulated role in matrix adhesion and migration (21,22), the *cellular adhesion molecule 1* (*ICAM1*), which is important for endothelial transmigration into tissues (23), and the matrix metalloproteinases *MMP1* and *MMP7*, both with crucial roles in migration and invasion (24–26). In this context, stably DKK2 silenced ES cells showed significantly reduced invasiveness when subjected to Matrigel-covered transwell assays (BioCoat^{TM} Angiogenesis System) (Fig. 4C). As previously reported MMPs seems to be important for ES invasiveness (18). Therefore, we examined the invasiveness of A673 and SK-N-MC cells after treatment with 3nM or 6nM Batimastat (BB-94) - a specific MMP inhibitor. As expected, treatment with BB-94 prominently reduced the amount of cells crossing the Matrigel (Fig. 4D). We next transiently knocked down MMP1 or MMP7, each with two different specific siRNAs. As demonstrated in Fig. 4E and 4F, only knock-down of MMP1, but not of MMP7, reduced invasiveness of ES cells, suggesting that the reduced invasive potential of DKK2 silenced ES cells is mediated - at least in part - via MMP1.

DKK2 decreases neuronal differentiation *in vitro*

Subsequent gene set enrichment analysis (GSEA) of our microarray data identified 75 differentially regulated gene sets (NES < -1.54 or NES > 1.30), that belong to one of the three ontologies: molecular function, cellular component or biological processes (C5: GO gene sets, v3.0; (27)). Set-to-set analysis of leading-edge top ranked down-regulated gene sets (C5_all, v3.0) revealed a strong over-

representation of gene sets involved in anti-apoptotic pathways (supplementary Fig. S2A-C), that possibly explains the slightly higher rate of dead cells after DKK2 knock-down *in vitro* and *in vivo* (Fig. 2D, sub-G1 fraction; data not shown). Consistently, DKK2 knock-down increased the rates of apoptosis as measured by annexin-V and 7-AAD staining (supplementary Fig. S2D). Moreover, the set-to-set analysis of the up-regulated gene sets (C5_all, v3.0) revealed a strong over-representation of gene sets involved in neuronal differentiation and development (Fig. 5A+B). To verify this prediction, we first examined the overexpression of three leading-edge genes, which are all involved in neurogenesis, namely *glial fibrillary acidic protein* (*GFAP*), *nerve growth factor receptor* (*NGFR*) and *slit, drosophila, homolog of, 2* (*SLIT2*) using qRT-PCR (Fig. 5C). Subsequently, we induced neurogenic differentiation with 0.1mM BHA in 2% DMSO in stable A673, SK-N-MC and TC-71 DKK2 shRNA infectants. We observed that ES cell lines were able to fully differentiate and express GFAP, a major intermediate filament protein of mature astrocytes (28), only after DKK2 suppression (Fig. 5D). Similarly growth-associated protein 43 (GAP43), a protein exclusively expressed on the synaptosomal membrane of nerve tissues (29), was significantly higher expressed in ES cells after DKK2 knock-down, as shown in Fig. 5E, indicating that DKK2 inhibits the neuronal differentiation potential of ES cells.

DKK2 enhances bone invasion and osteolysis *in vivo*

We next investigated whether DKK2 can influence their differentiation potential towards other tissues or lineages. Min *et al.* already demonstrated that DKK2 promotes angiogenesis (30), therefore, we examined the endothelial differentiation capacity of ES cells, but we did not detect any differences between cells with/without

DKK2 knock-down in tube formation assays (supplementary Fig. S3A+B). Moreover, given that DKK2 is also implicated in terminal osteoblast differentiation (14,16) and osteoclastogenesis (14,15), we subsequently analyzed the ability of ES cells to differentiate along bone lineages. As demonstrated in supplementary Fig. S4, induction of chondrogenic and osteogenic differentiation with specific growth media was clearly impaired in DKK2 knock-down cells. Furthermore, we examined the differential expression of key players associated with bone colonization in stable DKK2 infectants. We chose *chemokine, CXC motif, receptor 4* (*CXCR4*), *parathyroid hormone-like hormone* (*PTHrP*), *RUNT-related transcription factor 2* (*RUNX2*) and *transforming growth factor beta-1* (*TGFβ1*) for follow-up due to their involvement in preparing the pre-metastatic niche, homing and invasion to bone as well as their role in local and metastatic tumor growth in bones (26). We could demonstrate that the expression of these genes was significantly reduced in ES cells with constitutive DKK2 knock-down compared to controls (Fig. 6A). Interestingly, three of the five genes are also involved in the osteolytic behavior of tumor cells (26), which seems important since ES are well-known osteolytic tumors. To verify this observation, we further analyzed the expression of other genes associated with osteolysis, namely *hypoxia-inducible factor 1, alpha subunit* (*HIF1α*), *jagged 1* (*JAG1*), *interleukin 6* (*IL6*), *vascular endothelial growth factor receptor 1* (*VEGF*) (26). As expected, knock-down of DKK2 significantly reduced the expression of these genes (Fig. 6B)

Based on these results, we analyzed whether suppression of DKK2 has a role in the process of bone invasion and osteolysis *in vivo*. We injected constitutively DKK2 silenced A673 cells into the tibiae of immunodeficient $Rag2^{-/-}\gamma c^{-/-}$ mice and analyzed bone infiltration and destruction by X-ray radiography and histology. As shown in Fig. 6C-F, DKK2 knock-down significantly reduced bone infiltration and osteolysis. Only

25% of the mice injected with A673 pSIREN^{DKK2} cells exhibited an infiltration of tumor cells into bone, whereas bone invasion was observed in 87.5% of the respective controls (Fig. 6D). The pSIREN^{DKK2}-mediated lesions were smaller and less destructive than the lesions caused by control cells, as measured by the amount of TRAP positive osteoclasts in the tumor (Fig. 6E+F). In addition, pilot screening of human ES samples suggested the level of DKK2 expression to be associated with invasive growth and survival (supplementary Fig. S5), although a careful retrospective study here is necessary to obtain significant results.

In summary, these data demonstrate that DKK2 critically influences the differentiation process of ES cells along the chondrogenic and osteogenic lineage and is crucial for ES bone invasion and osteolysis *in vitro* and *in vivo*.

Discussion

ES are osteolytic bone tumors, characterized by early metastasis into lungs and bones (2). In the present study, we identified DKK2 as a highly overexpressed protein in ES that seems critically involved in the malignant behavior of this disease, presumably in part via the activation of Wnt/β-catenin signaling (supplementary Fig. S6). Our data support a role of DKK2 overexpression for the maintenance of ES osteolysis, bone invasiveness and metastatic spread, associated with a reprograming from neuronal to chondro-osseous differentiation. Furthermore, we demonstrated that DKK2 is also important for anchorage-independent colony formation and proliferation of ES cells *in vitro* and for tumorigenicity *in vivo*. High expression of DKK2 in ES raises the question whether DKK2 expression is dependent on the oncogenic fusion protein EWS-FLI1, as reported by Miyagawa *et al.* (31). However, in line with the findings of Navarro *et al.* (32), we found that the expression of DKK2 is mostly independent of EWS-FLI1.

Our functional analyses suggest that in ES MMP1 but not MMP7 is responsible for the reduced invasiveness after DKK2 knock-down *in vitro*. MMP1 as well as MMP7 are known to be involved in bone invasion and bone metastasis (24–26) although this finding does not preclude other DKK2 driven factors to be relevant for invasiveness and metastasis. One possible alternative candidate is E-Cadherin, a key cell-cell adhesion molecule, which is up-regulated after DKK2 knock-down and which has a strong anti-invasive and anti-metastatic role in tumor progression (20). In ES, it mainly seems to suppress anoikis through activation of *ERBB4*, however this gene is not enhanced after DKK2-mediated CDH1 increase (data not shown) (33). Other genes associated with invasion and metastasis, are suppressed after DKK2 knock-down such as *CD44* - an integral cell membrane glycoprotein. As CD44 promotes

cell proliferation, invasion and migration and further inhibits apoptosis, its down-regulation after DKK2 knock-down may in part explain the increase of cell death observed in our study (21,22,34). In addition, invasion in ES cells may also be promoted by the intercellular adhesion molecule 1 (ICAM1), which is important for the extravasation of circulating tumor cells during metastasis (23). Of note, four of our five validated DKK2 target genes are associated with bone colonization, bone invasion and osseous differentiation, which is interesting in the pathophysiological context of ES that frequently arise in and metastasize into bones.

In recent years some genes were identified, that enabled bone metastasis of different tumor entities. Among them are *secreted phosphoprotein 1* (*OPN*; (35)) a potent ligand of CD44 (22), *cbp/p300-interacting transactivator, with glu/asp-rich c-terminal domain, 2* (*CITED2*; (36)), *cAMP response element-binding protein 1* (*CREB1*; (37)) and *secreted protein, acidic, cysteine-rich* (*SPARC*; (38)). Interestingly, CD44 and OPN as well as the target genes of CITED2 (*MMP*s, *TGFβ1*, *PTHrP*), CREB1 (*MMP*s, *PTHrP*) and SPARC (*VEGF*) are also regulated by DKK2, as demonstrated in this study. Moreover, we showed that DKK2 modulates the expression of additional genes important for osteolysis (*CXCR4*, *HIF1α*, *JAG1*, *IL6*, *PTHrP* and *VEGF*). Furthermore, high CXCR4 expression seems associated with poor prognosis in ES patients (39). The transcription factor RUNX2 affects cancer cell invasion and osteolysis (26) and can bind to the oncogenic fusion protein EWS-FLI1 (40). This interaction is potentially fostered by a DKK2-dependent RUNX2 induction and thus promotes the differentiation of ES cells (40). This could explain the increased neuronal differentiation of ES cells after DKK2 knock-down demonstrating that not only EWS-FLI1 driven histone methyltransferase EZH2 influences the differentiation potential in ES (17). However, their chondrogenic and osteogenic differentiation capacity is reduced after DKK2 knock-down, which may be again mediated at least in

part by RUNX2 since this protein promotes osteogenic and chondrogenic differentiation (26,40,41). Furthermore, we could demonstrate for the first time that reduced osteolysis after DKK2 knock-down *in vivo* is probably mediated by decreased expression of osteolytic genes, which function either directly via the stimulation of osteoclastic bone resorption (PTHrP, IL6, VEGF) or indirectly (HIF1α, JAG1) by increasing the ratio of receptor activator of NF-κB ligand (RANKL) to osteoprotegerin (OPG) to activate the maturation of osteoclast precursors (26,42). These data in addition might be of clinical relevance since pilot data obtained from human ES immunohistology indicate the level of DKK2 expression to be associated with tumor invasiveness and survival.

In synopsis, the current study provides evidence that DKK2 is critically involved in ES pathology, especially in bone associated tumor growth and metastasis. With DKK2, we could identify a first element for the mechanisms of bone invasiveness and osteolysis in ES. DKK family members seem likely to be involved in other bone infiltrating tumors including osteosarcoma as well as breast or prostate cancer (43–45) supporting a critical role of Wnt/β-catenin signaling for bone metastasis. Hence, DKK2 may constitute a promising new drug target in different bone cancers and bone metastasis that can possibly be used to prevent or at least to delay metastasis.

Acknowledgements

We thank Colette Berns for expert technical assistance and Uwe Thiel for support and critically reading of the manuscript. Immunodeficient Rag2$^{-/-}\gamma c^{-/-}$ mice were kindly provided by Mamoru Ito (Central Institute for Experimental Animals).

References

1. Lessnick SL, Ladanyi M. Molecular pathogenesis of ewing sarcoma: new therapeutic and transcriptional targets. Annu Rev Pathol 2012;7:145–59.

2. Mackintosh C, Madoz-Gúrpide J, Ordóñez JL, Osuna D, Herrero-Martín D. The molecular pathogenesis of Ewing's sarcoma. Cancer Biol Ther 2010;9:655–67.

3. Ewing J. Classics in oncology. Diffuse endothelioma of bone. James Ewing. Proceedings of the New York Pathological Society, 1921. CA Cancer J Clin 1972;22:95–8.

4. Schmidt D, Harms D, Burdach S. Malignant peripheral neuroectodermal tumours of childhood and adolescence. Virchows Arch A Pathol Anat Histopathol 1985;406:351–65.

5. Burdach S, Jürgens H. High-dose chemoradiotherapy (HDC) in the Ewing family of tumors (EFT). Crit Rev Oncol Hematol 2002;41:169–89.

6. Burdach S, Thiel U, Schöniger M, Haase R, Wawer A, Nathrath M, et al. Total body MRI-governed involved compartment irradiation combined with high-dose chemotherapy and stem cell rescue improves long-term survival in Ewing tumor patients with multiple primary bone metastases. Bone Marrow Transplant 2010;45:483–9.

7. Coleman RE. Clinical features of metastatic bone disease and risk of skeletal morbidity. Clin Cancer Res 2006;12:6243s–6249s.

8. Staege MS, Hutter C, Neumann I, Foja S, Hattenhorst UE, Hansen G, et al. DNA microarrays reveal relationship of Ewing family tumors to both endothelial and fetal neural crest-derived cells and define novel targets. Cancer Res 2004;64:8213–21.

9. Katoh M, Katoh M. WNT antagonist, DKK2, is a Notch signaling target in intestinal stem cells: augmentation of a negative regulation system for canonical WNT signaling pathway by the Notch-DKK2 signaling loop in primates. Int J Mol Med 2007;19:197–201.

10. Brott BK, Sokol SY. Regulation of Wnt/LRP signaling by distinct domains of Dickkopf proteins. Mol Cell Biol 2002;22:6100–10.

11. Mao B, Niehrs C. Kremen2 modulates Dickkopf2 activity during Wnt/LRP6 signaling. Gene 2003;302:179–83.

12. Li L, Mao J, Sun L, Liu W, Wu D. Second cysteine-rich domain of Dickkopf-2 activates canonical Wnt signaling pathway via LRP-6 independently of dishevelled. J Biol Chem 2002;277:5977–81.

13. Uren A, Wolf V, Sun Y-F, Azari A, Rubin JS, Toretsky JA. Wnt/Frizzled signaling in Ewing sarcoma. Pediatr Blood Cancer 2004;43:243–9.

14. Fujita K, Janz S. Attenuation of WNT signaling by DKK-1 and -2 regulates BMP2-induced osteoblast differentiation and expression of OPG, RANKL and M-CSF. Mol Cancer 2007;6:71.

15. Tian E, Zhan F, Walker R, Rasmussen E, Ma Y, Barlogie B, et al. The role of the Wnt-signaling antagonist DKK1 in the development of osteolytic lesions in multiple myeloma. N Engl J Med 2003;349:2483–94.

16. Li X, Liu P, Liu W, Maye P, Zhang J, Zhang Y, et al. Dkk2 has a role in terminal osteoblast differentiation and mineralized matrix formation. Nat Genet 2005;37:945–52.

17. Richter GHS, Plehm S, Fasan A, Rössler S, Unland R, Bennani-Baiti IM, et al. EZH2 is a mediator of EWS/FLI1 driven tumor growth and metastasis blocking endothelial and neuro-ectodermal differentiation. Proc Natl Acad Sci U S A 2009;106:5324–9.

18. Grunewald TGP, Diebold I, Esposito I, Plehm S, Hauer K, Thiel U, et al. STEAP1 Is Associated with the Invasive and Oxidative Stress Phenotype of Ewing Tumors. Mol Cancer Res 2012;10:52–65.

19. Subramanian A, Tamayo P, Mootha VK, Mukherjee S, Ebert BL, Gillette MA, et al. Gene set enrichment analysis: a knowledge-based approach for interpreting genome-wide expression profiles. Proc Natl Acad Sci U S A 2005;102:15545–50.

20. Hanahan D, Weinberg RA. Hallmarks of cancer: the next generation. Cell 2011;144:646–74.

21. Aruffo A, Stamenkovic I, Melnick M, Underhill CB, Seed B. CD44 is the principal cell surface receptor for hyaluronate. Cell 1990;61:1303–13.

22. Weber GF, Ashkar S, Glimcher MJ, Cantor H. Receptor-ligand interaction between CD44 and osteopontin (Eta-1). Science 1996;271:509–12.

23. Roland CL, Harken AH, Sarr MG, Barnett CC Jr. ICAM-1 expression determines malignant potential of cancer. Surgery 2007;141:705–7.

24. Lynch CC, Hikosaka A, Acuff HB, Martin MD, Kawai N, Singh RK, et al. MMP-7 promotes prostate cancer-induced osteolysis via the solubilization of RANKL. Cancer Cell 2005;7:485–96.

25. Lu X, Wang Q, Hu G, Van Poznak C, Fleisher M, Reiss M, et al. ADAMTS1 and MMP1 proteolytically engage EGF-like ligands in an osteolytic signaling cascade for bone metastasis. Genes Dev 2009;23:1882–94.

26. Weilbaecher KN, Guise TA, McCauley LK. Cancer to bone: a fatal attraction. Nat Rev Cancer 2011;11:411–25.

27. Ashburner M, Ball CA, Blake JA, Botstein D, Butler H, Cherry JM, et al. Gene ontology: tool for the unification of biology. The Gene Ontology Consortium. Nat Genet 2000;25:25–9.

28. Reeves SA, Helman LJ, Allison A, Israel MA. Molecular cloning and primary structure of human glial fibrillary acidic protein. Proc Natl Acad Sci U S A 1989;86:5178–82.

29. Benowitz LI, Routtenberg A. GAP-43: an intrinsic determinant of neuronal development and plasticity. Trends Neurosci 1997;20:84–91.

30. Min J-K, Park H, Choi H-J, Kim Y, Pyun B-J, Agrawal V, et al. The WNT antagonist Dickkopf2 promotes angiogenesis in rodent and human endothelial cells. J Clin Invest 2011;121:1882–93.

31. Miyagawa Y, Okita H, Itagaki M, Toyoda M, Katagiri YU, Fujimoto J, et al. EWS/ETS regulates the expression of the Dickkopf family in Ewing family tumor cells. PLoS ONE 2009;4:e4634.

32. Navarro D, Agra N, Pestaña A, Alonso J, González-Sancho JM. The EWS/FLI1 oncogenic protein inhibits expression of the Wnt inhibitor DICKKOPF-1 gene and antagonizes beta-catenin/TCF-mediated transcription. Carcinogenesis 2010;31:394–401.

33. Kang H-G, Jenabi JM, Zhang J, Keshelava N, Shimada H, May WA, et al. E-cadherin cell-cell adhesion in ewing tumor cells mediates suppression of anoikis through activation of the ErbB4 tyrosine kinase. Cancer Res 2007;67:3094–105.

34. Park YS, Huh JW, Lee JH, Kim HR. shRNA against CD44 inhibits cell proliferation, invasion and migration, and promotes apoptosis of colon carcinoma cells. Oncol Rep 2012;27:339–46.

35. Bäuerle T, Adwan H, Kiessling F, Hilbig H, Armbruster FP, Berger MR. Characterization of a rat model with site-specific bone metastasis induced by MDA-MB-231 breast cancer cells and its application to the effects of an antibody against bone sialoprotein. Int J Cancer 2005;115:177–86.

36. Lau WM, Weber KL, Doucet M, Chou Y-T, Brady K, Kowalski J, et al. Identification of prospective factors promoting osteotropism in breast cancer: a potential role for CITED2. Int J Cancer 2010;126:876–84.

37. Son J, Lee J-H, Kim H-N, Ha H, Lee ZH. cAMP-response-element-binding protein positively regulates breast cancer metastasis and subsequent bone destruction. Biochem Biophys Res Commun 2010;398:309–14.

38. De S, Chen J, Narizhneva NV, Heston W, Brainard J, Sage EH, et al. Molecular pathway for cancer metastasis to bone. J Biol Chem 2003;278:39044–50.

39. Bennani-Baiti IM, Cooper A, Lawlor ER, Kauer M, Ban J, Aryee DNT, et al. Intercohort gene expression co-analysis reveals chemokine receptors as prognostic indicators in Ewing's sarcoma. Clin Cancer Res 2010;16:3769–78.

40. Li X, McGee-Lawrence ME, Decker M, Westendorf JJ. The Ewing's sarcoma fusion protein, EWS-FLI, binds Runx2 and blocks osteoblast differentiation. J Cell Biochem 2010;111:933–43.

41. Sugawara M, Kato N, Tsuchiya T, Motoyama T. RUNX2 expression in developing human bones and various bone tumors. Pathol Int 2011;61:565–71.

42. Sethi N, Dai X, Winter CG, Kang Y. Tumor-derived JAGGED1 promotes osteolytic bone metastasis of breast cancer by engaging notch signaling in bone cells. Cancer Cell 2011;19:192–205.

43. Hoang BH, Kubo T, Healey JH, Yang R, Nathan SS, Kolb EA, et al. Dickkopf 3 inhibits invasion and motility of Saos-2 osteosarcoma cells by modulating the Wnt-beta-catenin pathway. Cancer Res 2004;64:2734–9.

44. Bu G, Lu W, Liu C-C, Selander K, Yoneda T, Hall C, et al. Breast cancer-derived Dickkopf1 inhibits osteoblast differentiation and osteoprotegerin expression: implication for breast cancer osteolytic bone metastases. Int J Cancer 2008;123:1034–42.

45. Hall CL, Bafico A, Dai J, Aaronson SA, Keller ET. Prostate cancer cells promote osteoblastic bone metastases through Wnts. Cancer Res 2005;65:7554–60.

Table/Figure Legends

Table 1: Total number of apparent metastases

Quantitative evaluation of metastasis: All macroscopically visible metastases in lungs, livers and kidneys were counted and confirmed by histology after injection with A673 pSIREN^{negsiRNA} or pSIREN^{DKK2} cells, respectively.

Figure 1: DKK2 is highly overexpressed in Ewing sarcomas

(**A**) Expression profile of DKK2 in ES in comparison to normal tissue (NT) and fetal tissue (FT). ES and NT samples were analyzed using EOS-Hu01 microarrays (8) (**B**) DKK2 expression in different tumor cell lines analyzed by qRT-PCR. Data are mean ± SEM. (**C**) RNA interference of EWS-FLI1 expression (bottom) does not suppress DKK2 RNA expression (top). EWSFLI1_2 represents the specific siRNA (neg.control: non silencing siRNA). Results of qRT-PCR 48 hours after transfection were shown. Data are mean ± SEM of two independent experiments; t-test. NTC: non template control. (**D**) Analysis of DKK2 and EWS-FLI1 expression after constitutive DKK2 knock-down using qRT-PCR. Data are mean ± SEM of two independent experiments; t-test. NTC: non template control.

Figure 2: DKK2 knock-down influences *in vitro* growth

(**A**) Transient transfection of ES cell lines with different specific siRNAs. Knock-down efficacy was tested by qRT-PCR 72 hours after transfection. Data are mean ± SEM of three independent experiments; t-test. NTC: non template control. (**B**) Constitutive suppression of DKK2 expression after infection of ES cells with DKK2 specific

shRNA constructs as measured by qRT-PCR and Western blot analysis (pSIREN^{DKK2}, control: pSIREN^{negsiRNA}). qRT-PCR data are mean ± SEM of 20 independent experiments; t-test. NTC: non template control. (**C**) Left; analysis of proliferation of constitutively infected ES cell lines with xCELLigence. Cellular impedance was measured every 4 hours (relative cell index). Data are mean ± SEM (hexaplicates/group); t-test. Right; doubling time of constitutive A673 and SK-N-MC DKK2 shRNA infectants. Data are mean ± SEM of two independent experiments/cell line (hexaplicates/group); t-test. (**D**) Summary of two independent cell cycle distribution analyses of shRNA infectants by propidium iodine staining and flow cytometry. (**E**) Analysis of anchorage-independent colony formation in methylcellulose of ES cell lines with stable DKK2 knock-down (pSIREN^{DKK2}). Left, macrographs show a representative experiment with TC-71. Right, data are mean ± SEM of three independent experiments (duplicates/group); t-test.

Figure 3: **DKK2 increases local tumor growth and metastasis *in vivo***

(**A**) Left; evaluation of tumorigenicity of constitutive A673 and SK-N-MC DKK2 shRNA infectants in immunodeficient mice (3-5 mice/group). Right; post *ex vivo* DKK2 expression using qRT-PCR. Data are mean ± SEM, t-test. (**B**) Analysis of metastatic potential of A673 and SK-N-MC with stable DKK2 knock-down and controls (pSIREN^{negsiRNA}; 4 mice/group). The top two panels demonstrate lung with extensive metastases (arrow) and the bottom two panels depict lung without metastases after A673 pSIREN^{DKK2} injection (H&E; scale bar 5mm or 2mm).

Figure 4: **DKK2 knock-down suppresses invasiveness regulated by MMP1**

(**A**) Microarray data of selected genes after transient DKK2 knock-down (GSE36100). (**B**) Confirmation of the array results for selected genes presumably influencing invasiveness with constitutive DKK2 knock-down infectants using qRT-PCR. (*CDH1*, *CD44*, *ICAM1*, *MMP1*, *MMP7*, *DKK2*). Data are mean ± SEM of three independent experiments; t-test. NTC: non template control. (**C**) Analysis of invasiveness of ES cell lines through Matrigel after transfection with specific DKK2 shRNA constructs. Data are mean ± SEM of two independent experiments; t-test. (**D**) Analysis of invasiveness of A673 and SK-N-MC treated with 3 or 6nM of the MMP-inhibitor Batimastat (BB-94) or vehicle. Data are mean ± SEM of two independent experiments; t-test. (**E+F**) Invasiveness of A673 and SK-N-MC after transfection with two specific MMP1 (5F) or MMP7 (5E) siRNAs 48 hours before seeding. Data are mean ± SEM; t-test.

Figure 5: **DKK2 knock-down increases neuronal differentiation**

(**A**) GSEA leading edge analysis of identified gene sets up-regulated by transient DKK2 knock-down (GSEA; C5_all, GO gene sets). Set-to-set analysis shows a correlation between DKK2 knock-down and up-regulation of neuronal differentiation genes. (NES: normalized enrichment score). (**B**) GSEA enrichment plot of one representative gene set after constitutive suppression of DKK2. (**C**) qRT-PCR of different neuronal marker genes after stable DKK2 knock-down. (*GFAP*, *NGFR, SLIT2*, *DKK2*). Data are mean ± SEM of two independent experiments; t-test. NTC: non template control. (**D**) Analysis of neurogenic differentiation of stable A673 infectants pSIREN^{DKK2} and pSIREN^{negsiRNA} treated for 6 days with 0.1mM BHA. Immunofluorescent staining of GFAP is shown (scale bar 500µm). Similar results

were obtained with SK-N-MC and TC-71. (**E**) Evaluation of the differentiation potential after neurogenic differentiation of ES cell lines constitutively transfected with DKK2 shRNA treated for 6 days with 0.1mM BHA shown by Western blot analysis with GAP43 antibody and corresponding densitometrie (top). Hypoxanthine guanine phosphoribosyltransferase (HPRT) was used as loading control.

Figure 6: **DKK2 enhances bone invasiveness and osteolysis**

(**A**) qRT-PCR of ES cell lines with stable DKK2 knock-down. (*CXCR4*, *PTHrP*, *RUNX2, TGFβ*, *DKK2*). Data are mean ± SEM of three independent experiments; t-test. NTC: non template control. (**B**) mRNA expression analyses of known osteolytic genes after constitutive DKK2 knock-down using qRT-PCR. (*HIF1α*, *IL6*, *JAG1*, *VEGF*, *DKK2*). Data are mean ± SEM of two independent experiments; t-test. NTC: non template control. (**C-F**) Analysis of bone invasiveness and osteolysis of constitutive A673 DKK2 shRNA infectants and negative controls in an orthotopic bone xenotransplantation model (9 mice/group). Affected bones were assessed by X-ray radiography and histology. (**C**) A673 pSIREN^{DKK2} cells caused significantly less tumor infiltration into bone when compared to A673 pSIREN^{negsiRNA}, where tumor cells destroyed the cortical bone (arrows) and generated extra tumor mass outside the bone (X-ray, H&E; scale bar 0.25mm). (**D**) Percentage of mice exhibiting bone infiltration after intra-tibial injection. Data are mean ± SEM; t-test (*$p < 0.01$). (**E**) TRAP staining of osteoclasts to quantify osteolysis. (scale bar 0.25mm and 0.05mm (insets)). (**F**) Average number of TRAP^{+} osteoclasts (1mm^2) (3 tumor samples/group; t-test).

Table 1: Total number of apparent metastases

	total number of apparent metastases			
	A673		SK-N-MC	
	pSIREN^{negsiRNA}	pSIREN^{DKK2}	pSIREN^{negsiRNA}	pSIREN^{DKK2}
liver	12	2	135	8
lung	366	14	0	0
kidney	2	0	0	0

Quantitative evaluation of metastasis: All macroscopically visible metastases in lungs, livers and kidneys were counted and confirmed by histology after injection with A673 pSIREN^{negsiRNA} and pSIREN^{DKK2} cells.

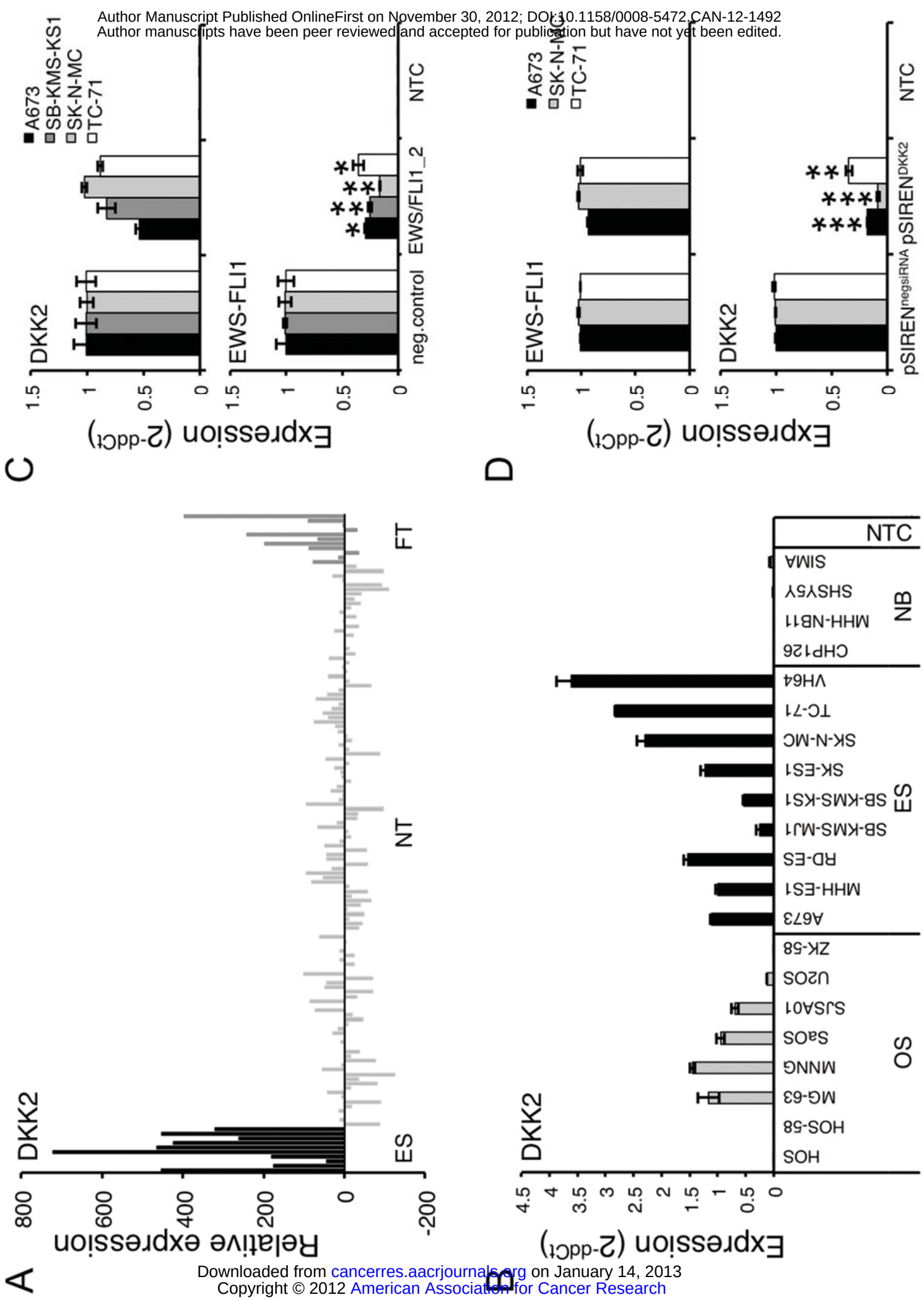

Fig. 1

Fig. 2

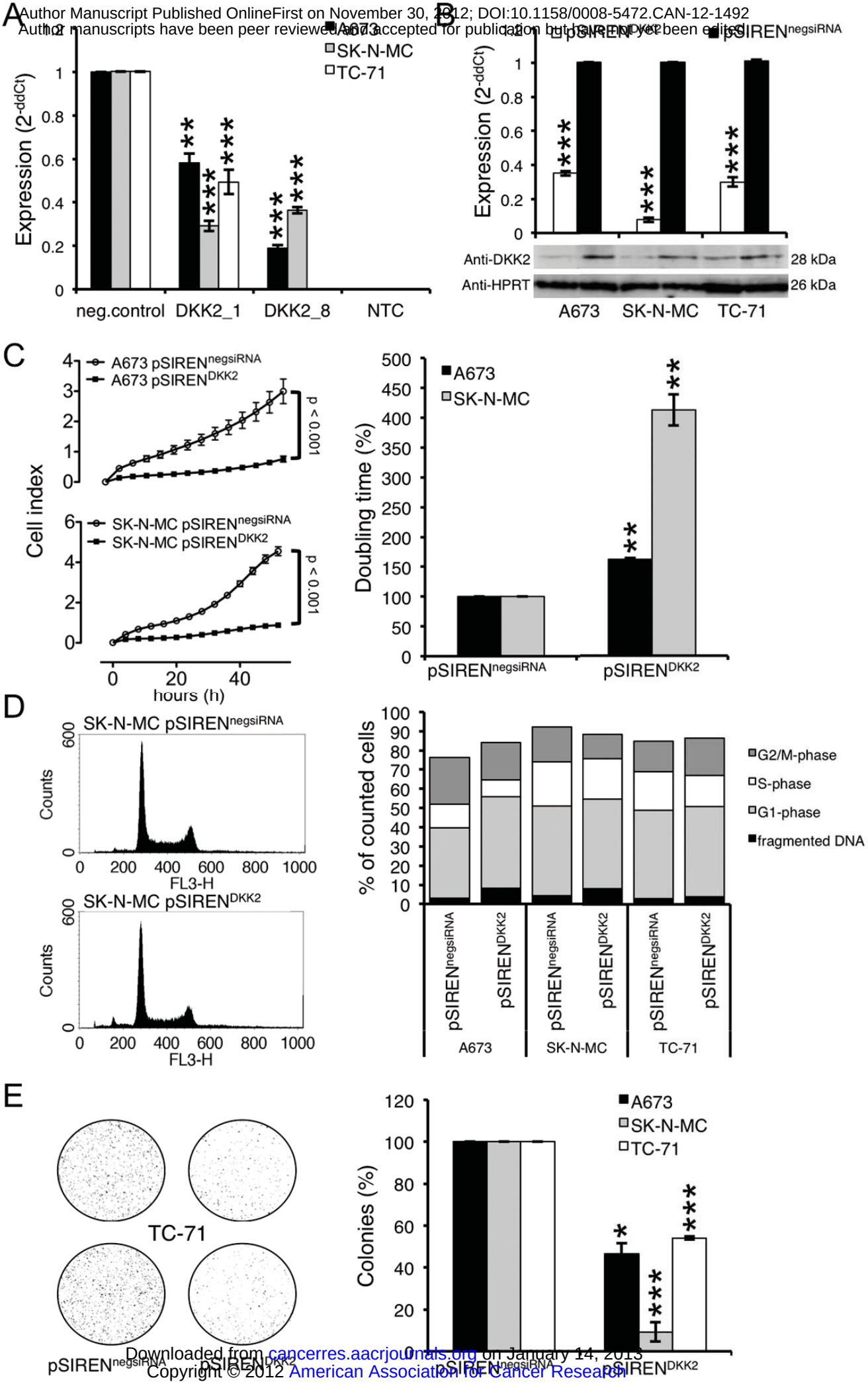

Fig. 3

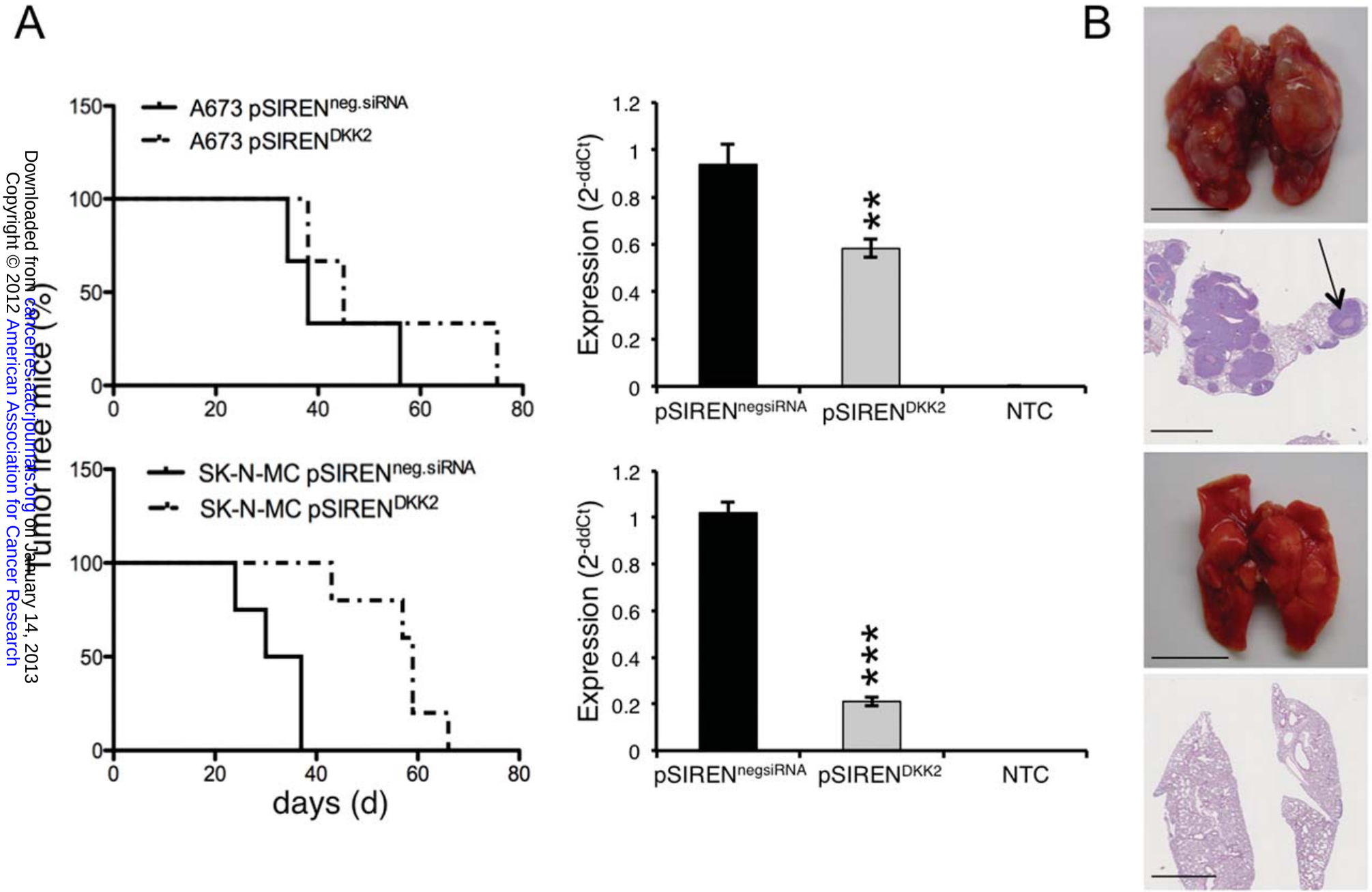

Fig. 4

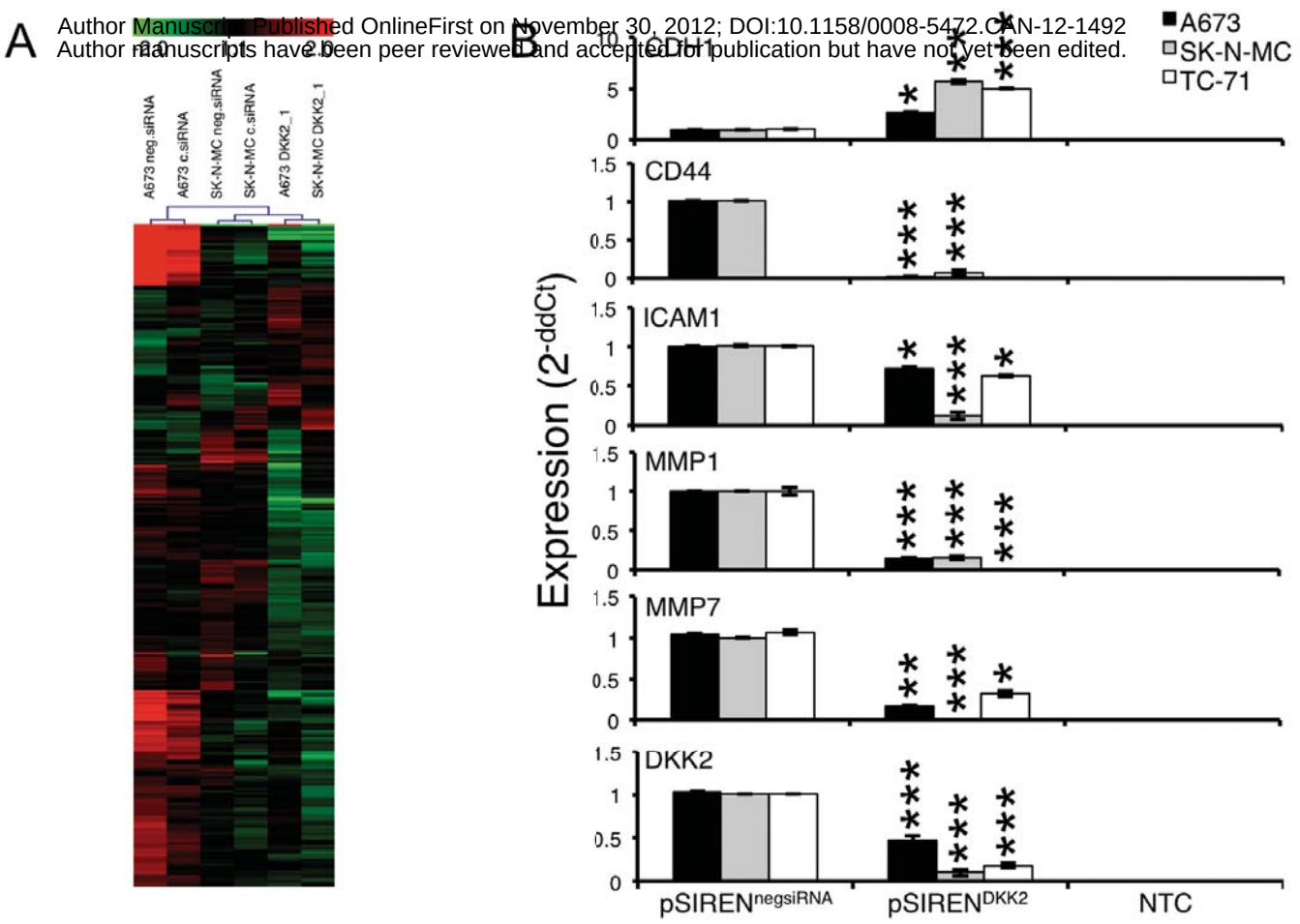

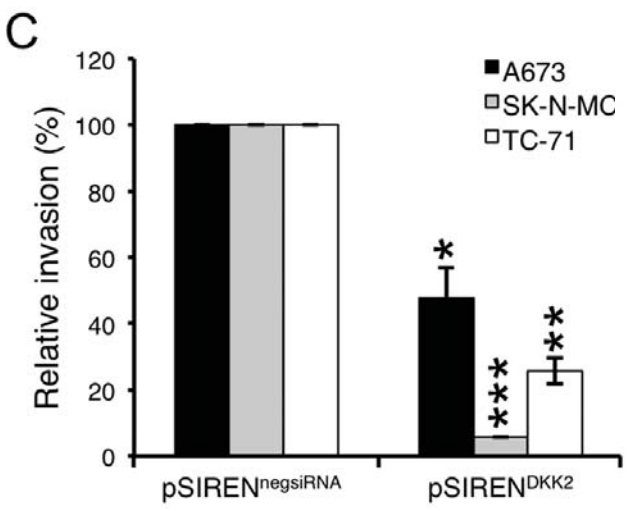

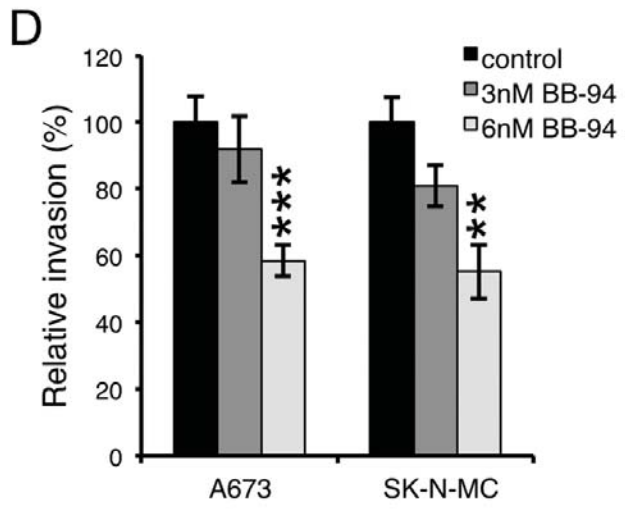

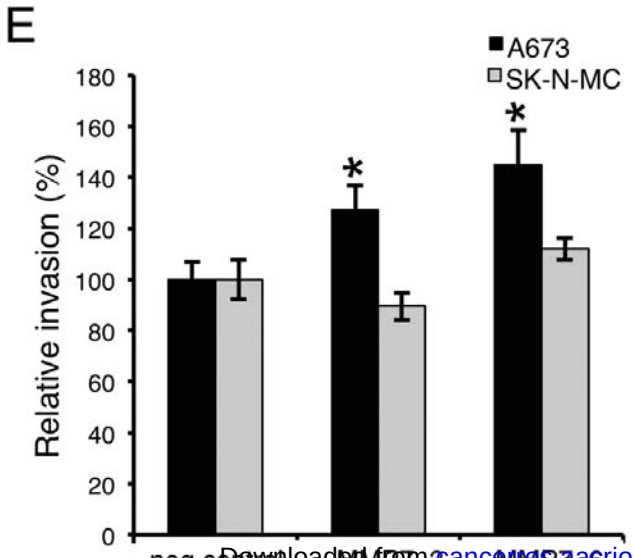

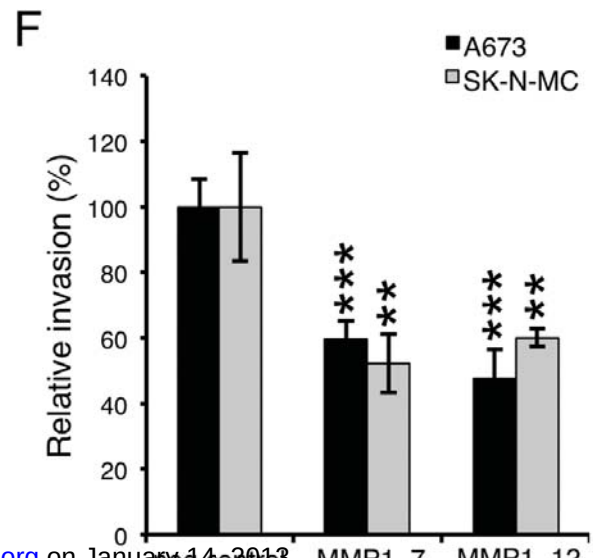

Author Manuscript Published OnlineFirst on November 30, 2012; DOI:10.1158/0008-5472.CAN-12-1492
Author manuscripts have been peer reviewed and accepted for publication but have not yet been edited.

A

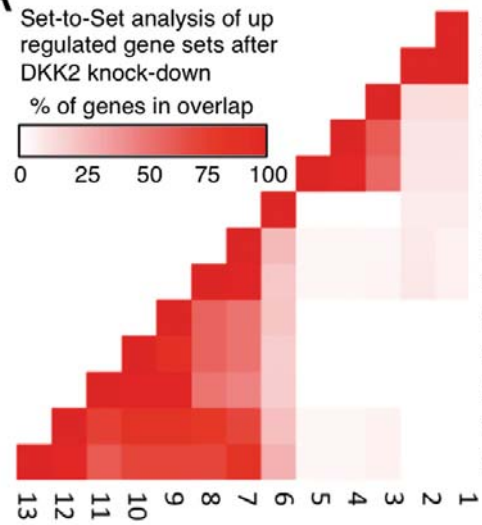

	pathway name	NES	p
1	synaptic transmission	1.63	0.00
2	transmission of nerve impulse	1.59	0.00
3	metal ion transport	1.65	0.01
4	cation transport	1.51	0.01
5	ion transport	1.46	0.01
6	nervous system development	1.47	0.00
7	generation of neurons	1.55	0.02
8	neuron differentiation	1.45	0.04
9	neurite development	1.54	0.01
10	axonogenesis	1.68	0.01
11	cellular morphogenesis during development	1.48	0.05
12	neuron development	1.64	0.01
13	neurogenesis	1.38	0.03

B

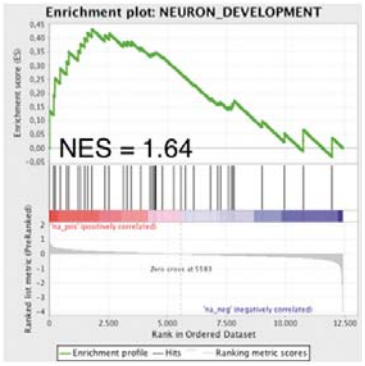

C

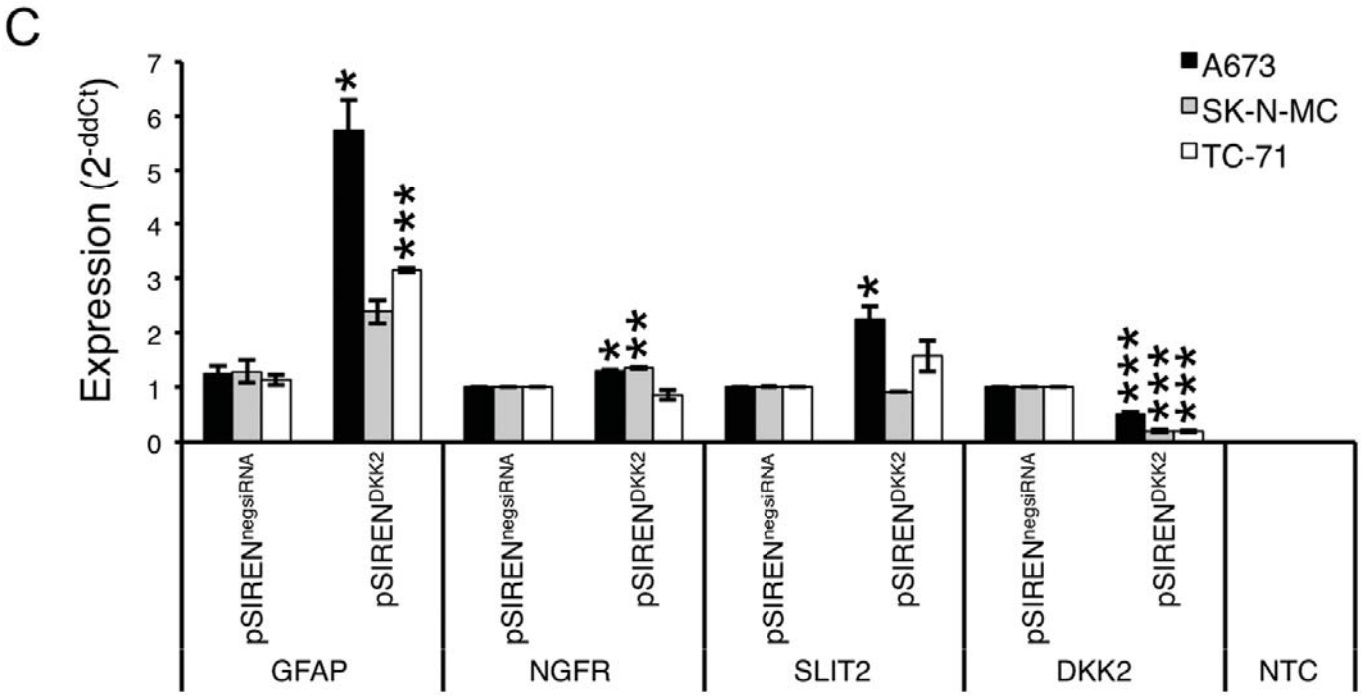

D

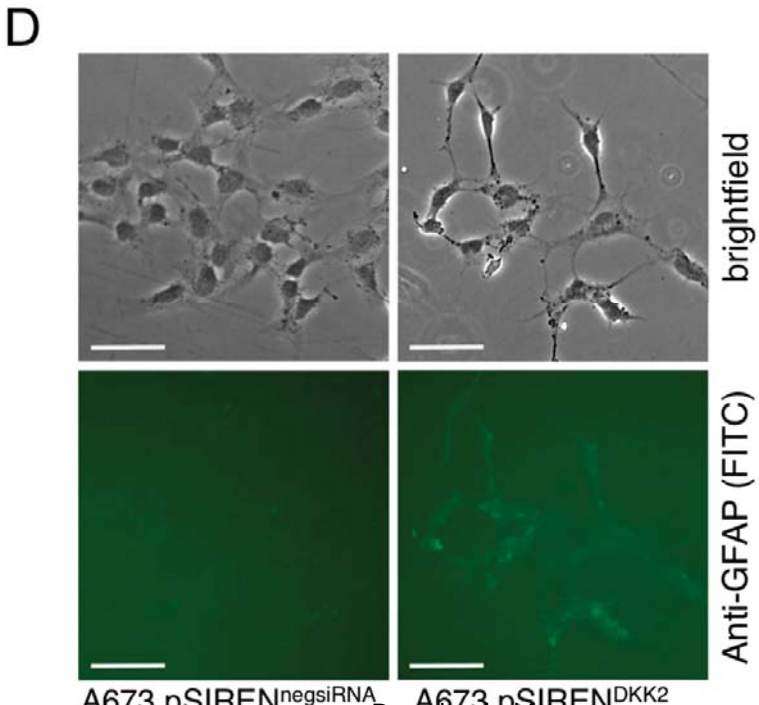

E

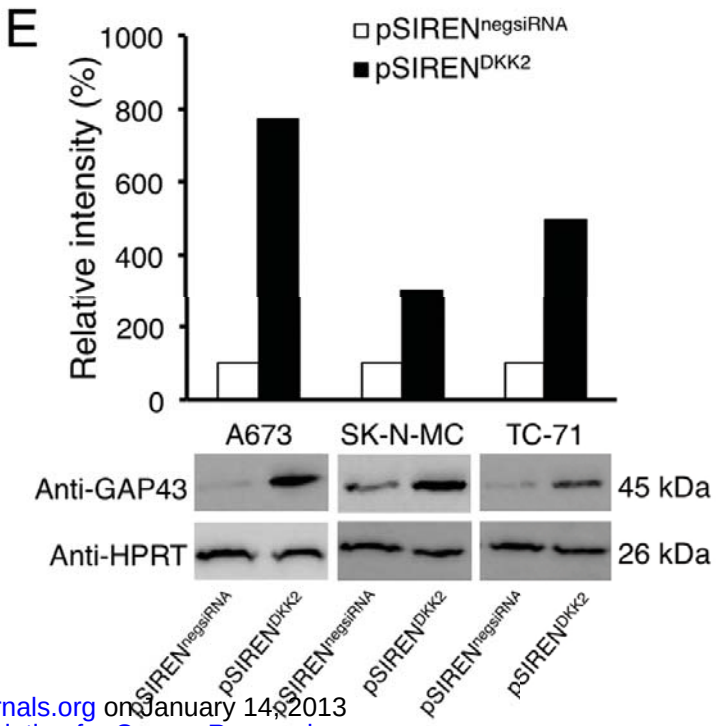

Author Manuscript Published OnlineFirst on November 30, 2012; DOI:10.1158/0008-5472.CAN-12-1492
Author manuscripts have been peer reviewed and accepted for publication but have not yet been edited.